Ocean Front Detection From Instant Remote Sensing SST Images

Yuting Yang, Junyu Dong, Xin Sun, *Member, IEEE*, Redouane Lguensat, *Student Member, IEEE*, Muwei Jian, and Xinhua Wang

***Abstract*— Identifying fronts manually from satellite images is a tedious and subjective task. Accordingly, edge detection algorithms are introduced for automatic detection of fronts. However, traditional algorithms cannot be applied to cloud-contaminated images, because missing data caused by occasional cloud coverage interferes with front detection. To diminish this risk, this letter proposes a new algorithm for a quick and an accurate detection of fronts from an instant cloud-contaminated sea surface temperature (SST) image, instead of depending on the daily or weekly averaged SST images. This algorithm adopts a data-driven analog interpolation method, which estimates missing values from the historical data of the same region. After reducing the contour between the interpolated data and the original data, an instant front detection algorithm is proposed based on microcanonical multiscale formalism (MMF). The algorithm utilizes MMF to detect singularity exponents (SEs), and then enhances the features detected in a cloud-contaminated region. Finally, a threshold is set to extract fronts from SE. Experimental results on an AVHRR satellite SST image of 12:00 o'clock covering China Coastal waters confirmed the effectiveness of the proposed algorithm.**

***Index Terms*— Analog data assimilation, microcanonical multiscale formalism (MMF), sea surface temperature (SST), thermal fronts.**

I. Introduction

CLOUD contamination is a classic problem for object recognition from remote sensing images. To diminish the risk of cloud contamination, numerous front detection algorithms were proposed based on weekly or daily averaged remote sensing images [12]. This letter proposes a new algorithm for a quick and an accurate detection of objects (i.e., ocean fronts) from an instant cloud-contaminated sea surface temperature (SST) image, without depending on the averaged intensity values over multi-instant images. Ocean fronts can be defined as relatively narrow zones of enhanced horizontal gradients of hydrographic properties that separate broader areas of different vertical structures, and are often associated with mixing and enhancing biological production. Knowledge of thermal fronts is an important factor in various ocean-related fields, such as fisheries and global warming. In particular, thermal fronts represent a key geophysical parameter for constraining the exchange of energy and moisture between the ocean and the atmosphere [14].

Transitions of gray level values inside complex natural images, such as SST images, indicate the existence of intermittency and a multiscale organization characteristic of fully developed turbulence (FDT) [4]. Microcanonical multifractal formalism (MMF) focuses on the multiscale structure characteristic of FDT, which is too complicated to obtain satisfactory results by conventional (linear) approaches, such as gradient-based algorithms [2] and histogram analysis algorithms [9]. Unlike "canonical" approaches that rely on large ensemble averages and ergodic hypothesis, MMF is not associated with "thermalized" values, which have flaws dealing with empirical data [13]. Instead, in a microcanonical analogy, the behavior of the measure is evaluated locally and geometrically at every given pixel location, without relying on thermalized averages [7].

In this letter, we propose a two-mission instant front detection algorithm, concretely, missing data interpolation for the region under clouds, and front detection on instant SST images. The data-driven analog interpolation method [5] is introduced to fill in missing data in SST images caused by cloud contamination. Then, based on the MMF algorithm, we further apply fronts enhancement method in the resulting singularity exponent (SE) image so as to refine the fronts in the cloud-contaminated region.

Our contribution consists in proposing a framework aiming at solving the scientific problem of detecting ocean fronts in instant cloud-contaminated SST images. First, the framework uses an interpolation method to estimate the missing data based on historical SST images. This is the basic condition of detecting the fronts under clouds. However, the resolution of the interpolated data is relatively low, so we have to enhance the features in the interpolation region. Second, this framework then adopts an MMF method to detect fronts in instant cloud-contaminated SST images. The MMF is a powerful tool for front detection in uncontaminated SST images. Nevertheless, when encountered with cloud-contaminated images, the performance of MMF is barely satisfactory. In an instant cloud-contaminated SST image, most of the fronts adjacent to the cloud had to be abandoned, but now the problem has been solved with the proposed MMF method.

Manuscript received June 27, 2016; revised September 10, 2016; accepted October 14, 2016. Date of publication November 21, 2016; date of current version December 7, 2016. This work was supported in part by the National Natural Science Foundation of China under Grant 41576011, Grant 61401413, and Grant 61601427, in part by the Natural Science Foundation of Shandong Province under Grant ZR2014FQ023 and Grant ZR2015FQ011, and in part by the Opening Fund of State Key Laboratory of Applied Optics. *(Corresponding author: Xin Sun and Junyu Dong.)*

Y. Yang, J. Dong, X. Sun, and M. Jian are with the Department of Computer Science and Technology, Ocean University of China, Qingdao 266100, China (e-mail: sunxin@ouc.edu.cn; dongjunyu@ouc.edu.cn).

R. Lguensat is with the Department of Signal and Communications, Institut Mines-Telecom/ Telecom Bretagne, 29200 Brest, France.

X. Wang is with the State Key Laboratory of Applied Optics ,Changchun Institute of Optics, Fine Mechanics and Physics, Chinese Academy of Sciences, Changchun, Jilin 130033, China.

Color versions of one or more of the figures in this letter are available online at http://ieeexplore.ieee.org.

Digital Object Identifier 10.1109/LGRS.2016.2618941

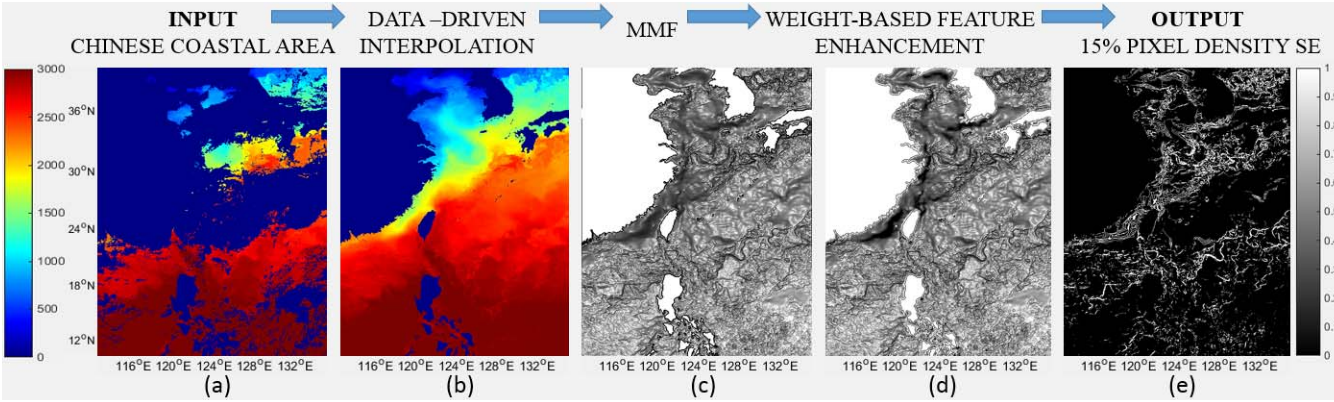

Fig. 1. Simplified block diagram of the automatic algorithm used to detect the thermal upwelling structures in SST images. (a) AVHRR daily SST images. (b) Interpolation image. (c) SE image. (d) Enhanced SE image. (e) Extracted fronts image.

The remainder of this letter is organized as follows. Section II presents the methodology proposed in this letter. Section III describes the experimental data and analyzes the experimental results. Finally, the conclusion is drawn in Section IV.

II. Methodology

Cloud-contaminated regions are often called sparse data regions. Sparse data regions are typically caused by scattered clouds and traditional front detection algorithms cannot be applied in these regions. Hence, the key point of the proposed algorithm lies in that the sparse data regions should be unveiled, i.e., interpolated.

The classical approaches to interpolate SST data rely on spatial or spatiotemporal optimal kriging interpolation algorithms [3]. When considering parametric covariance models, the calibration of the covariance model and the associated stationarity hypothesis are the complex issues. Other methods, such as ensemble Kalman filtering methods [6], exhibit long execution time which can represent an undesirable issue in our application, while methods based on empirical orthogonal functions (EOFs) [1] lack clear accounting of temporal dependency. For these reasons and aiming for a proof of concept, we adopted a data-driven analog interpolation method in this letter because of its simplicity and effectiveness. This method presented in Lguensat *et al.* [5] states missing data interpolation as a data assimilation issue and presents a fully data-driven strategy for the reconstruction of missing data in remote sensing observation series by exploiting a hidden Markov model (HMM) formulation.

As shown in Fig. 1, the proposed algorithm follows five steps. The first step is to fill in missing values of the original image. The original image is shown in Fig. 1(a) (the blue color with value 0 stands for the cloud and the land); meanwhile, the interpolated image is shown in Fig. 1(b). In the second step, an MMF method is proposed to calculate the SEs in the interpolated image, as shown in Fig. 1(c). However, SE image might contain some undesirable contours on the boundary between the original data and the interpolated data. Thus, in the third step, a Gaussian 3×3 filter is applied to smooth the boundary. Then, fronts enhancement method is applied in the missing data region. The enhanced SE image is shown

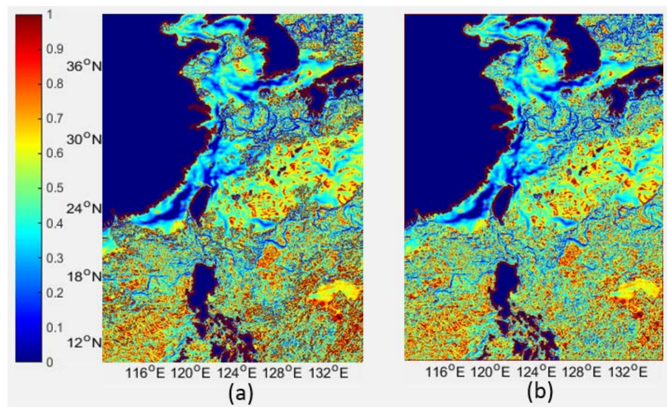

Fig. 2. (a) SE image with contour. (b) SE image without contour.

in Fig. 1(d). Finally, the fronts are extracted from enhanced SE image with a pixel density of 10%. The extracted fronts image is shown in Fig. 1(e). The following paragraphs provide a detailed description of each of the aforementioned steps.

A. Step 1 (Interpolation Method)

The interpolation method estimates hidden variables (the interpolated images) from the observed variables (images with missing data). For this aim, an HMM framework is designed, where the following holds.

1) The discrete state values $(z_i)_i$ of the Markov Chain refer to the different elements of the catalog $\mathcal{C}$ of historical images of the same region. The problem being of high dimension, we consider that their EOF projections (it is also called principal component analysis) result in lower dimensional states, compared with the observations.
2) Transition probabilities $(A = \{a_{ij}\} = P(X_t = z_j | X_{t-1} = z_i))$ are evaluated using an "Analog Forecasting" idea: for every state z_i, we search for its K-nearest neighbors in the catalog and consider their successors in time. The probabilities are then only evaluated from z_i to these K successors. As an example, let us suppose state z_i have the analog z_{ai} and z_j is the successor of z_{ai}, then the transition probability a_{ij} from z_i to z_j is evaluated as follows:

$$a_{ij} \propto \exp(-\lambda \|z_i - z_{ai}\|) \tag{1}$$

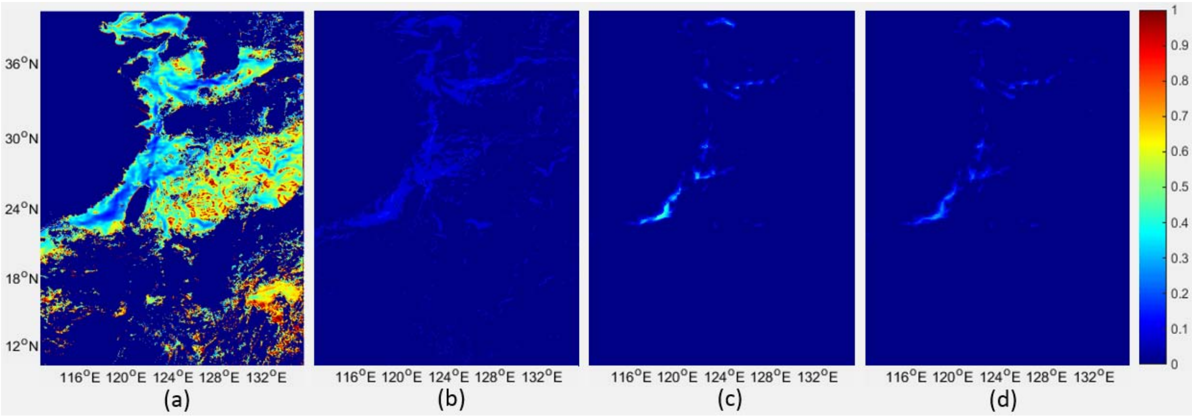

Fig. 3. (a) Interpolated region. The enhanced feature images are obtained using different window groups denoted as (b)–(d), respectively. These groups are (b) 5×5 window, 7×7 window, and 9×9 window, (c) five nearest neighbors window, 3×3 window, and 5×5 window, and (d) two directional three nearest neighbors window, five nearest neighbors window, and 3×3 window.

where λ is a scaling parameter to be the median of distances $\|z_i - z_{ai}\|$. The number of nearest neighbors K is tuned in a cross-validation step and is set to 10.

3) Emission probabilities ($B = \{b_j(Y_t)\} = P(Y_t|X_t = z_j)$) follow a Gaussian observation model.

Estimation of interpolated SST images is then performed using the classical forward–backward algorithm presented in the tutorial of Rabiner [11]. The algorithm combined with analog forecasting ideas estimates the posteriors given a sequence of observations and is called in [5] by the analog forward–backward algorithm.

B. Step 2 (Contour Smooth Method)

While the original data are taken from an instant SST image, the interpolated data make use of historical SST images. Thus, there can be difference between the interpolated data and the original data, i.e., the pixel values shift on the boundary between the interpolated data and the original data. Once the front detection algorithm is applied in such an image, a contour between the interpolated data and the original data, as shown in Fig. 2(a), will create fake fronts and affect the result's validity.

Corresponding solution consists in determining the boundary position, applying a Gaussian 3×3 filter to the boundary. After this processing operation, the contours will be greatly reduced, as shown in Fig. 2(b).

C. Step 3 (MMF Method)

To calculate SE, we utilize a novel formalism called the MMF, which is based on the strength of variations between nearby pixels of SST images. Since the range of the variations can be determined according to the size of the oceanography characteristics, physical processes, such as fronts and eddies, can be easily detected with MMF.

The key point in MMF is the proper determination of SE value $h(\overrightarrow{x})$. In this context, an approach presented in [10] provides numerically stable computation of SE value at each pixel, based on the wavelet projection of the measure

$$h(\overrightarrow{x}) = \frac{\log\left(\frac{\tau_\psi \mu(\overrightarrow{x}, r_0)}{<\tau_\psi \mu(., r_0)>}\right)}{\log r_0} + o\left(\frac{1}{\log r_0}\right). \tag{2}$$

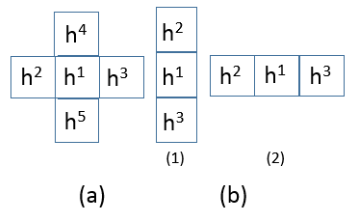

Fig. 4. (a) Five nearest neighbors window. (b) Two directional three nearest neighbor window. 1: transverse three nearest neighbor window. 2: longitudinal three nearest neighbor window.

The scale r_0 is used for image normalization, given an image with the size $N \times M$ corresponds to size 1, so that $r_0 = 1/(N \times M)$. $\tau_\psi \mu(., r_0)$ is chosen as the average value of the wavelet projection over the whole signal. Accordingly, $\tau_\psi \mu(x, r_0)$ corresponds to the wavelet projection at point x. A fraction of the smallest SE, also known as the most singular manifold (MSM), indicates the highest strength of variations among the pixels in the SST image. Furthermore, given the intermittency and the existence of multiscale organization, the MSM is composed of the most unpredictable points, i.e., the least values of SE. The MSM is defined as

$$F_\infty = \overrightarrow{x} : h(\overrightarrow{x}) = h_\infty = \min(h(\overrightarrow{x})). \tag{3}$$

D. Step 4 (Front Enhancement Method)

The proposed fronts enhancement method is in order to improve the accuracy of front extraction. More distinct differentiation between the values of SE will be calculated to determine which part of SE belongs to fronts. In this step, a group of sliding windows will be applied across the image to obtain statistical information at each pixel. Then, the statistical information will be used as a weight to update SE value at that point. As a result, part of SE originally belonging to fronts are not considered as fronts now if the updated SE values are beyond the threshold range. The determination of the threshold range will be discussed in Section III.

The equation of this method is simplified as follows:

$$h_2(\overrightarrow{x}) = \frac{h_1(\overrightarrow{x})}{w_2(\overrightarrow{x})}. \tag{4}$$

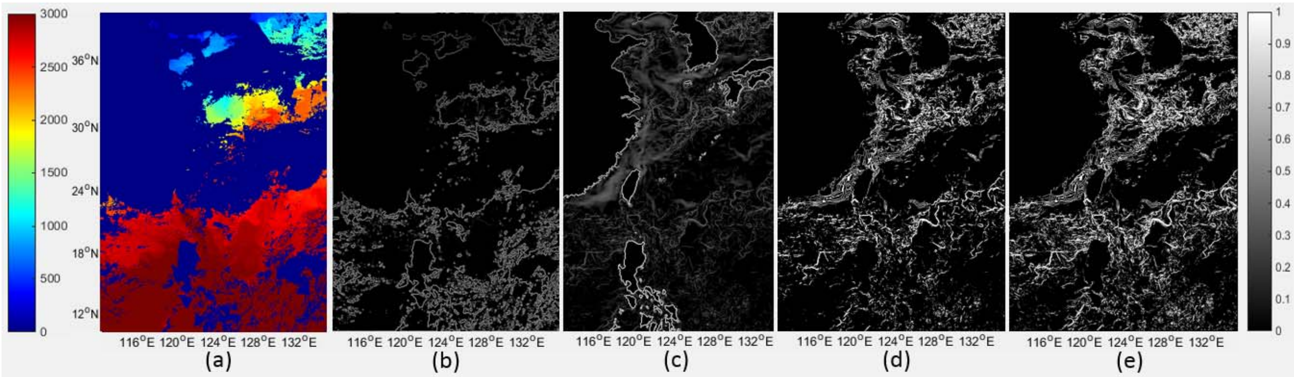

Fig. 5. (a) Instant SST image, the blue region contains cloud and land. (b) SE detected using MMF in SST image without interpolation. (c) SE detected using the proposed MMF method in interpolated SST image. Front images extracted from SE with pixel density of (d) 10% and (e) 15%, respectively.

Algorithm 1 Fronts Enhancement Method

1: **Input:** a small fraction of SE within window i centred at the position (m, n)
2: **for** i=1 to 3 **do**
Calculate the average SE value in the current window $\frac{\sum_{j=1}^{s^i}(h_1^j(\vec{x}))}{s^i}$
Count the number c_{mn} of $h_1^j(\vec{x})$ within the threshold range
The weight for window i at point $\vec{x}$ is obtained by $w_{mn}^i(\vec{x})$
3: **end for**
The average weight for the three window is $w_2(\vec{x})$
The updated SE is then achieved as $h_2(\vec{x}) = \frac{h_1(\vec{x})}{w_2(\vec{x})}$
4: **Output** $h_2(\vec{x})$

Given a point $\vec{x}$ in SE image, $h_1(\vec{x})$ gives the original value of the point, $h_2(\vec{x})$ corresponds to the updated value of the point, and $w_2(\vec{x})$ is the weight corresponding to the point

$$w_{mn}^i = \frac{\frac{\sum_{j=1}^{s^i}(h_1^j(\vec{x}))}{s^i} * s_1}{c_{mn} * h_1(\vec{x})}, \quad i = 1, 2, 3. \tag{5}$$

The weight $w_{mn}^i(\vec{x})$ is calculated based on a small fraction of SE within window i centered at the position (m, n). c_{mn} is the number of SE within a threshold range. The value of s_1 is four-fifths of the window size s^i, $s_1 = 4 * s^i/5$

$$w_2(\vec{x}) = \frac{\sum_{i=1}^{3}(w_{mn}^i(\vec{x}) * s^i)}{\overline{s}} \tag{6}$$

where $w_2(\vec{x})$ is the average weight value of $w_{mn}^i(\vec{x})$ achieved in each of the three windows. $\overline{s}$ is the average window size. The overall fronts enhancement method is given in Algorithm 1.

E. Step 5 (Front Extraction Method)

However, the fronts extracted from the interpolated data are still too rough to determine the exact location in contrast with the fronts extracted from the original data. The proposed solution is to extract the skeleton S^i of the fronts from the interpolated data with different pixel densities p^i, respectively, and the threshold range is faithfully determined according to pixel density. Finally, S, the combination of fronts skeletons within each pixel density, is available for further upgrading the accuracy of the fronts in cloud-contaminated region

$$S = \sum_{i=1}^{5} \frac{i}{(S^i(H(p^i)))} \tag{7}$$

where $H(p^i)$ is a small fraction of SE within a threshold range defined by the parameter p^i, which is set according to pixel density, 2%, 4%, 6%, 8%, and 10%, respectively.

III. Experimental Results and Discussion

A. Study Area and Data

In this letter, we make use of a database of 600 daily averaged AVHRR SST images covering China coastal waters from January 1st to April 10th during the six years from 2007 to 2012 as historical data, and one AVHRR SST image taken at 12:00 o'clock in February 2013 with a resolution of $1/20° \times 1/20°$ covering China coastal waters (112.5E-135E,10N-40N) as the experiment data. This region, belonging to the Kuroshio Current system, transports enormous amounts of mass and energy (e.g., heat) from low to midlatitude regions [15].

B. Results and Analysis

As a comparison with the chosen window group, the window group of 3 × 3, 5 × 5, and 7 × 7 could only extract rough features, as shown in Fig. 3(b). Even through it contains most of the fronts, it could not meet the requirements in terms of fronts accuracy. When a smaller window group of two directional three nearest neighbors, five nearest neighbors, 3 × 3 is applied, most of the fronts are lost, leaving a small fraction of precise fronts, as shown in Fig. 3(d), which is not a satisfying situation either. For the fronts enhancement method, as shown in Fig. 4, the window group employed in this experiment is a five nearest neighbor window, a 3 × 3 window, and a 5 × 5 window. The reason of choosing this window group is that this group could enable us to extract precise fronts without losing too much features compared with other window groups, as shown in Fig. 3(c).

As a comparison with the proposed algorithm, we apply the algorithm of [8] to an SST image, as shown in Fig. 5(a). The resulting SE image is shown in Fig. 5(b). Due to the existence of scattered cloud that interferes with front detection, the fronts in the result image could hardly be recognized. The disadvantage of their method is that they do not take the cloud-contaminated data into account. Their solution is to discard the fronts adjacent to cloud to ensure the effectiveness of their method. Compared with Fig. 5(b), the SE detected by our method, as is shown in Fig. 5(c), includes both the fronts in cloud-free region and the fronts under cloud.

Thresholds are then applied to $\min(h(x))$ to extract significant fronts. The threshold range extends from a low threshold (θ_L) to a high threshold (θ_H). The pixels which values are higher than θ_H or lower than θ_L will be set to zero. This procedure will reduce both the SE on the boundary line between the land and the ocean which values are lower than θ_L, and the SE that would not be regarded as fronts which values are higher than θ_H. θ_H and θ_L are determined by pixel density. The pixel density for θ_L is usually set to be 1%. This setting will filter out most of the boundary lines, meanwhile retain the ocean fronts. In order to satisfy different requirements, we set different pixel densities for θ_H. In addition, the density of the smallest SE is often set to be less than 20%. To enhance the persuasiveness of the result, we only choose 10% smallest SE in the cloud-contaminated region as the fronts, whereas, in the region without cloud, the pixel density is 15% and 20%, as shown in Fig. 5(d) and (e), respectively.

IV. Conclusion

In this letter, we propose a two-mission front detection algorithm, aiming at solving two scientific problems by order: the interpolation of missing data and detection of fronts. First, a data-driven analog interpolation method is introduced to fill in missing data in an instant SST image due to cloud coverage before front detection. Second, an MMF method is applied to an instant SST image to detect fronts. After that, a fronts enhancement method is proposed to refine the ocean fronts in the cloud-contaminated region. In the future, we will enhance the continuity of fronts near the boundary between the interpolated data and the original data, and increase the resolution of the interpolated image through improving the interpolation method.

References

[1] J.-M. Beckers, A. Barth, and A. Alvera-Azcárate, "DINEOF reconstruction of clouded images including error maps—Application to the sea-surface temperature around Corsican island," *Ocean Sci.*, vol. 2, no. 2, pp. 183–199, 2006.

[2] I. M. Belkin and J. E. O'Reilly, "An algorithm for oceanic front detection in chlorophyll and SST satellite imagery," *J. Marine Syst.*, vol. 78, no. 3, pp. 319–326, Oct. 2009.

[3] R. Daley, *Atmospheric Data Analysis*, vol. 2. Cambridge, U.K.: Cambridge Univ. Press, 1993.

[4] U. Frisch and R. J. Donnelly, "Turbulence: The legacy of A. N. Kolmogorov," *Phys. Today*, vol. 49, no. 11, pp. 521–523, 1995.

[5] R. Lguensat, P. Tandeo, P. Ailliot, B. Chapron, and R. Fablet, "Using archived datasets for missing data interpolation in ocean remote sensing observation series," in *Proc. OCEANS*, Shanghai, China, Apr. 2016, pp. 1–5.

[6] R. Lguensat, P. Tandeo, R. Fablet, and R. Garello, "Spatio-temporal interpolation of sea surface temperature using high resolution remote sensing data," in *Proc. Oceans-St. John's*, Sep. 2014, pp. 1–4.

[7] S. K. Maji and H. M. Yahia, "Edges, transitions and criticality," *Pattern Recognit.*, vol. 47, no. 6, pp. 2104–2115, Jun. 2014.

[8] A. Tamim *et al.*, "Detection of Moroccan coastal upwelling fronts in SST images using the microcanonical multiscale formalism," *Pattern Recognit. Lett.*, vol. 55, pp. 28–33, 2015.

[9] K. Nieto, H. Demarcq, and S. McClatchie, "Mesoscale frontal structures in the Canary upwelling system: New front and filament detection algorithms applied to spatial and temporal patterns," *Remote Sens. Environ.*, vol. 123, no. 6, pp. 339–346, Aug. 2012.

[10] O. Pont, A. Turiel, and H. Yahia, "Singularity analysis of digital signals through the evaluation of their unpredictable point manifold," *Int. J. Comput. Math.*, vol. 90, no. 8, pp. 1693–1707, 2013.

[11] L. Rabiner, "A tutorial on hidden Markov models and selected applications in speech recognition," *Proc. IEEE*, vol. 77, no. 2, pp. 257–286, Feb. 1989.

[12] H. Song, B. Huang, Q. Liu, and K. Zhang, "Improving the spatial resolution of landsat TM/ETM+ through fusion with SPOT5 images via learning-based super-resolution," *IEEE Trans. Geosci. Remote Sens.*, vol. 53, no. 3, pp. 1195–1204, Mar. 2015.

[13] H. Song, G. Wang, and K. Zhang, "Multiple change detection for multispectral remote sensing images via joint sparse representation," *Opt. Eng.*, vol. 53, no. 12, p. 123103, Dec. 2014.

[14] L. L. Stowe, A. P. Davis, and E. P. McClain, "Scientific basis and initial evaluation of the CLAVR-1 global clear/cloud classification algorithm for the advanced very high resolution radiometer," *J. Atmos. Ocean. Technol.*, vol. 16, no. 6, pp. 656–681, 2010.

[15] Y.-H. Tseng, M.-L. Shen, S. Jan, D. E. Dietrich, and C.-P. Chiang, "Validation of the Kuroshio current system in the dual-domain Pacific Ocean model framework," *Prog. Oceanogr.*, vol. 105, no. 5, pp. 102–124, Oct. 2012.